Springback adjustment for multi-point forming of thick plates in shipbuilding

Se Yun Hwang, Jang Hyun Lee *, Yong Sik Yang, Mi Ji Yoo

Department of Naval Architecture and Ocean Engineering, Inha University, Inchon, 402-751, Republic of Korea

ARTICLE INFO

ABSTRACT

At most shipyards, flame bending has been widely used to fabricate curved shells. Since residual deformation of flame bending is produced by thermo-elastic–plastic strains, it is difficult to accurately achieve the desired shape. Therefore, mechanical bending processes such as multi-press forming and multi-point press forming have become attractive because such processes can accurately control the desired shape. Springback is one of the major problems associated with mechanical bending. When the pressing tools are removed after the loading stage, the workpiece springs back due to the elastic recovery and the shape deviation needs to be compensated. The tools of the press forming process therefore need to be changed in order for the produced surface to reach the desired shape accurately after springback. Generally, forming tools are designed and constructed to operate through an iterative process in which the die and the pistons are adjusted to compensate for springback after a pressing operation. Such adjustments require significant time and effort. Therefore, the present study investigates not only how to simulate springback deformation, but also the degree of adjustment required to the stroke of pistons in multi-press forming. Finite Element Analysis (FEA) of thick metal forming and an iterative displacement adjustment algorithm are integrated for practical application. Shape deviations between the design surface and the deformed plate are minimized to reach the desired shape.

© 2010 Elsevier Ltd. All rights reserved.

1. Introduction

Generally, the objective of the design of a hull form in a marine vessel is to obtain a hull surface with minimum resistance to meet the required dead weight. The geometry of the hull surface is represented by a complex surface. Thereafter, the hull surface is divided into several hundred surface pieces according to the hull-block assembly and the lines of weld joints. In general, more than 50%–70% of the surface pieces are grouped into the curved surface with a double curvature. In most shipyards, the plates with double curvature are deformed from flat plates by flame bending (or line heating) or sequential roll-press forming and flame bending. However, the flame bending process is mostly dependent on the skill of experienced workers because of its complexity in the thermo-elastic–plastic deformation generated by the moving flame. Heating information such as the location of heating lines, sequence of lines, speeds, and maximum temperature have been determined by workers who have several years of experience. Also, flame bending needs to be carried out for several hours to obtain the desired shape since the heat source moves on many lines. Therefore, over the past 40 years many shipyard engineers and scholars have made numerous studies to develop an automation technique for

line heating [1,2]. Such studies have not only included the thermal-elastic–plastic behavior of the line heating process but also the automation of the process. The first attempt to simulate line heating was performed based on a simplified model [3,4]. Throughout the 1990s, many researchers investigated FEM to calculate the residual deformation generated by line heating [2,5]. Over the past 9 years, a number of practical systems [6–8] have been carried out for the automation of line heating processes. Tango et al. [6] developed an integrated system that carries out line heating automatically. The system, called IHI-Alpha, calculates a heating plan which includes the speed and electric current of induction heating. Park et al. [9] proposed a geometric assessment method in order to establish a theoretical foundation for the automation of line-heating. They focused on measurement, comparison, and the measurement data process in the overall system which was developed for the Samsung Heavy Industry Co., Ltd.

Despite a powerful simulation technique of flame bending, basic studies are still being conducted on the line heating process since the mechanism for line heating is too complicated to obtain accurate control. There is an urgent need for the development of the automation of the forming of curved surfaces.

Compared with flame bending, cold forming can reduce the production time even though it requires significant hydraulic power to form a thick plate. It is well known that die forming is useful for the mass-production of products such as automobiles or consumer goods. However, the fixed die is not suitable for shipbuilding because each hull piece differs. Also, there is no control

---

* Corresponding author. Tel.: +82 32 860 7345; fax: +82 32 864 5850.
E-mail addresses: jh_lee@inha.ac.kr, janghyunlee@gmail.com (J.H. Lee).
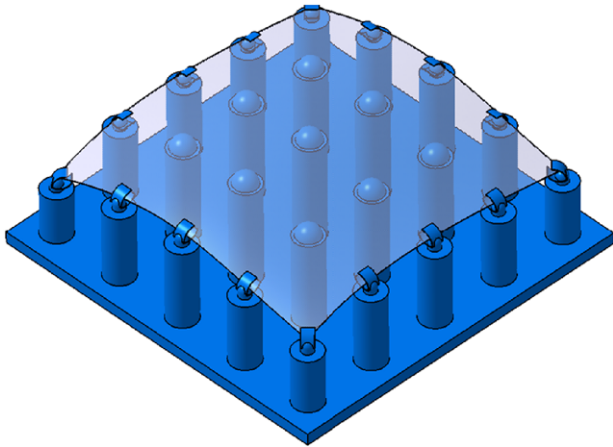
Fig. 1. Schematic view of multi-press forming machine.

in the forging process because of the thickness of the hull plates (generally over 12 mm). On the other hand, with the advantage of die-less forming, re-configurable press forming, and multi-point forming, cold forming is an attractive process in many shipyards. The forming system using reconfigurable press technology is a flexible tooling system for the automatic fabrication of arbitrary 3D surface parts [10]. In addition to the inherent flexibility of plate thicknesses, cold forming can form a variety of intricate shell shapes in shipbuilding within a short period of time. Therefore, cold forming technology has been considered in several shipyards as a way to overcome the difficulties associated with traditional line heating [11]. Since 2006, STX Offshore & Shipbuilding Co., Ltd. (STX shipyard) has been investigating cold forming methods that are adequate for shipbuilding. Evaluating the cold bending methods, i.e. multi-press, multi-point dieless forming, and multi-point press forming, the STX shipyard has designed a multi-point press forming (MPPF) device that has a reconfigurable discrete die to form thick plates that have large dimensions. The MPPF is a single-sided reconfigurable-die device with 9 inner rods and 16 edge constraint rods. Inner pressing rods are reconfigured by hydraulic movement in combination with pressing rods in edge constraints. The three-dimensional pressing value for the workpiece should be converted to NC data and downloaded to the machine controller of hydraulic presses that have freedom of movement along the $X–Y$ plane on the guide lines. Through an investigation of the maximum height of the hull pieces extracted from design data of containers, the maximum height of strokes of the punches was designed for manufacturing plates of any size. The in-plane movement of the plates is allowed because the projected area of the plate after the forming process on the initial plane of the plate is smaller than the initial area of the plate before processing. The schematic configuration of the MPPF equipment is illustrated in Fig. 1. The aim of the present study is to provide the MPPF equipment developed by the STX shipyard with a method to calculate the strokes of each pressing punch.

However, there are still a number of key technological problems that need to be solved for automatic dieless multi-point forming. Springback is one of the major problems of MPPF as it is with other mechanical bending methods. When the presses are released after the forming stage, the plate springs back due to elastic recovery [12]. Because the geometric tolerances can be tight for hull plate assembly, this shape deviation can become unacceptable. Springback can also make it difficult to approach the desired design shape at the first forming. The desired shape can, however, be efficiently achieved by an iterative process of bending and compensation. Therefore, springback compensation is necessary so that the punches of a multi-point press are adjusted such that the manufactured plate becomes geometrically accurate.

Redesigning or adjusting the tools manually to achieve the design shape for the manufactured plate is a time consuming process. Furthermore, because a hull surface is assembled from several hundreds of pieces of curved plate, an integrated system is required in order to automatically calculate the adjusted piston strokes.

Several completely automatic springback compensation algorithms have been reported and tested in previous studies [11–15]. The algorithm of the Displacement Adjustment (DA) method uses the shape deviation between the manufactured product and the desired shape, multiplied with modifying factors on each of the piston points, as a compensation function for the geometry of the tools. The advantages of the DA method are that the modification of the controlled stroke can also be carried out with a finite element analysis (FEA), and that it is possible to control the algorithm automatically.

The goal of this paper is to develop an integrated system that can automatically perform the springback compensation process and the calculation of piston strokes. Taking into consideration the predicted shape obtained by FEA, iterative displacement adjustment modifies the offset of pressing punches. We select the DA algorithm specifically applied to the bending of thick plate. FEA and the DA are incorporated in an integrated system so that the system can iteratively calculate the compensated geometry of a multi-point press. Here, a surface with a limited set of points is used to compare and evaluate the desired product shape and the unfolded shape, and to modify the strokes. For the practical application of this method, a program system has been developed to automatically offset the strokes of punches for the MPF procedure.

2. Data procedure in multi-point forming

2.1. Geometric data flow in multi-point forming

Generally, fitting and fairing the lines drawn from the data of ship offsets is often the beginning of the ship hull design procedure. The hull design procedure defines the surface of the ship hull, which approximates the points belonging to the hull [16]. Welding lines of the seam and butt are defined on the hull surface according to the plan of the block division. Thereafter, the hull surface is divided into many pieces that will be developed or unfolded into the two-dimensional (2D) flat pieces. The design surfaces are first trimmed from the three dimensional surface of the hull form. Thereafter, the pieces are unfolded onto the flat plates [17]. For most of the pieces, flame bending or press bending is applied to produce the desired shape. The schematic data flow of the desired surface and unfolded surface in the hull plate design is explained in Fig. 2.

For the application of multi-point forming, the initial stroke of each press is obtained from the displacement difference between the curved design surface and the flat unfolded surface. The frame coordinate of the design surface extracted from the computer-aided design (CAD) of a ship differs from that of the unfolded surface calculated by the unfolding module, for which a preprocessing step for surface matching, such as 'surface registration' or 'localization', is required [18–22]. Having two sets of point data, a surface matching process in which geometric shapes are represented by sparse points is then carried out, and the difference between pressing points is calculated through surface matching by a combination of the iterative closest Point (ICP) algorithm and the localization algorithm suggested in various studies [18–22].

Sparse points on the desired surface are taken, and a corresponding set of points on the unfolded surface is determined. Comparing the displacement difference between the unfolded surface and the design surface, the initial stroke of each press is determined. Fig. 3 introduces in detail the overall process of the
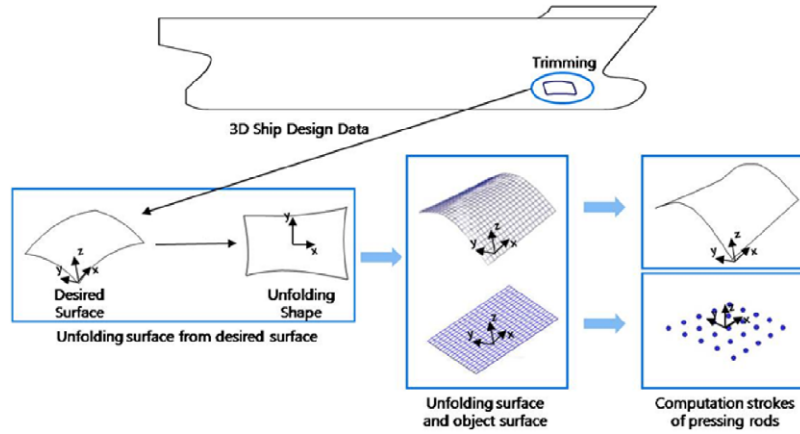
Fig. 2. Data flow of desired surface and unfolded surface in hull piece design.
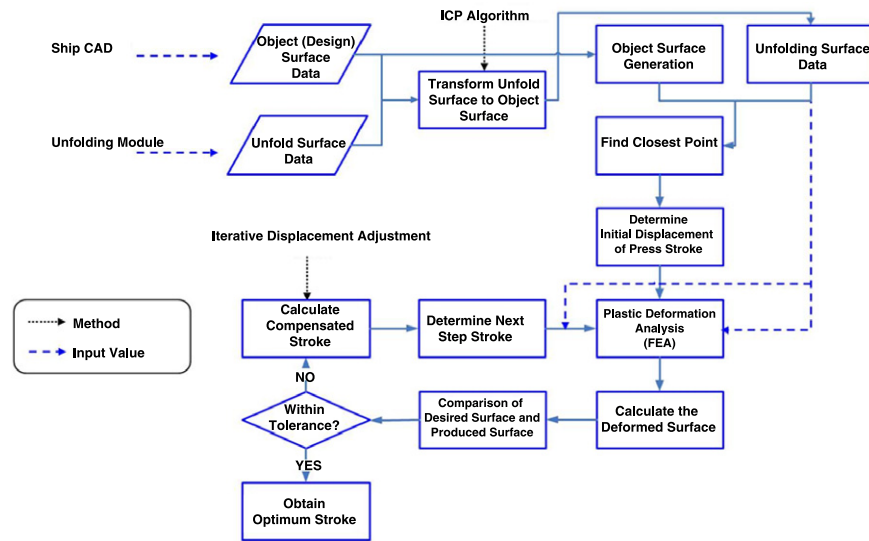
Fig. 3. Schematic process to determine the compensated stroke of press.

extraction of surfaces, the role of the ICP algorithm, and the determination of the amount of springback compensation. The surface registration describes the rotation and translation matrix to fit the unfolding surface for the desired surface. The ICP approach to register the surfaces is reported in various studies [18–22] and is thus not detailed in this paper. Displacement Adjustment accounts for the offset of the pressing tool in conjunction with the deformation prediction. First, the object surfaces and unfolded surfaces are matched together via the ICP method. Second, the initial offset or stroke of the pressing tool is directly assumed from the object surface. With these offset conditions, elastic–plastic analysis is performed. Third, the compensated offset is applied again to the analysis until the produced surface meets the desired surface. After the procedures have been completed, the offset is fastened to the pressing tools.

2.2. Representation of surface geometry

The design surface extracted from the ship CAD and the unfolded surface are identified as sets of points. When the design surface and unfolded surface data have been collected as sparse points, they are useful for making a surface representation to manipulate the required data for computation. Surface representation is particularly required to express the boundary points and inner points on the produced surface and unfolded surface. The explicit polynomial surface is taken into consideration for an efficient representation of the surfaces in this paper. Although parametric models such as Bezier, B-Spline, or Nonuniform Rational B-Spline (NURBS) are generally used for the representation of a surface in a geometric process, the polynomial equation is sufficient to extract the boundary points and inner points as well as to generate the finite element meshes for the spring back compensation. The polynomial function $D(x, y)$ for independent variables (x, y) of degree (k, k) can express the surfaces expressed as

$$z = D(x, y) = \sum_{i=0}^{k} \sum_{j=0}^{k} a_{ij} x^j y^j \tag{1}$$

where a_{ij} is a coefficient of each polynomial term.

Since the values of points (x_i, y_i, z_i) are generated from the desired surfaces and measured points, the polynomial surfaces were interpolated to the given sets of points. We evaluate the polynomial surfaces for degrees (2, 2), (3, 3), and (4, 4) by comparing the interpolated points obtained from the polynomial surface with those from the desired surface. We found that the cubic polynomial of the (3, 3) degree showed good agreement. The polynomial function can satisfy $z_i = D(x_i, y_i)$ for m data points (x_i, y_i, z_i) given, and the formulations are described by a

matrix form. Introducing the coefficients, $a_1, a_2, \ldots, a_{16}$ which are rearranged from a_{ij}, Eq. (1) can be transformed to a matrix form as follows in Eq. (2). It is possible to calculate the coefficients by introducing the given m data points.

The interpolation coefficients are obtained by easy calculation as follows:

$$(\mathbf{N}^T\mathbf{N})\,\mathbf{a} = \mathbf{N}^T\mathbf{q} \tag{2}$$

where $\mathbf{N}$ is a matrix expressed by the given data points of (x_i, y_i), $\mathbf{a}$ is a coefficient vector of the polynomial, and $\mathbf{q}$ is a vector of z_i at the given data points. These are represented as follows:

$$\mathbf{N} = \begin{bmatrix} x_1^3 & x_1^3 y_1 & \cdots & 1 \\ x_2^3 & x_2^3 y_2 & \cdots & 1 \\ \vdots & \vdots & \vdots & \vdots \\ x_m^3 & x_m^3 y_m & \cdots & 1 \end{bmatrix} \tag{3}$$

$$\mathbf{a} = \{a_1, a_2, \ldots, a_{16}\}^T \tag{4}$$

$$\mathbf{q} = \{z_1, z_2, \ldots, z_m\}^T. \tag{5}$$

2.3. Stroke of punches

The ICP algorithm and localization algorithm are used for geometric alignment and registration of three-dimensional surface models, as described in the previous section. The algorithm starts with two surfaces, the design surface and the unfolded surface, and iteratively determines the transformation by considering pairs of corresponding points on the surfaces and minimizing the distance between the design surface and the unfolded surface. According to the displacement distance, points on the flat unfolded surface adjust the strokes of the pressing punches. The punches are arranged between the unfolded surface and the design surface. The point of the curved piece is projected onto the point on the flat piece, and the correspondence stroke is assumed based on a point-to-point distance. As stated earlier in Fig. 1, the pressing machine has nine pressing rods in the inner region of the workpiece and sixteen pressing rods along the constraint edges. Hydraulic pressures are used for all rods so that the inner rods push the plate and the edge rods pull the plate.

Therefore, the initial stroke $\mathbf{c}_i$ that will be imposed on the ith point of the unfolded flat surface can be easily assumed by:

$$\mathbf{c}_i = \mathbf{r}_i - \mathbf{u}_i \tag{6}$$

where $\mathbf{r}_i$ and $\mathbf{u}_i$ denote the vertical offset of points on the desired shape and the location of the pressing punch, respectively. The points of the workpiece are projected onto the desired surface and the corresponding points can be easily obtained.

However, the head of the rod makes contact with the workpiece as the punch is pressed with the above initial stroke. To determine the vertical locations of punches, it is necessary to determine the relative position of each punch. The relative position of the rod should be determined by the contact point as seen in the side view shown in Fig. 4, since the punches' spherical head will always contact the workpiece at a tangency point and not at a center point.

Considering the contact configured by the radius (r) of the punch head and the workpiece thickness (t), the stroke of the punch can be modified as shown in Fig. 4. Cai and Li [23] suggested a non-linear equation to calculate the contact points and the position coordinate of pressing punches for sheet forming. Their non-linear equation was selected for this present study and an incremental scheme was used to calculate the contact point.

The incremental process can be summarized as follows:

1. Determining the location of the contact point of the punch head on the surface.
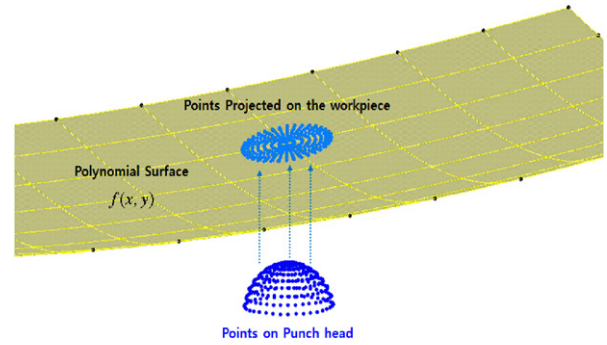
Fig. 4. Determining the relative contact position of punch's head.
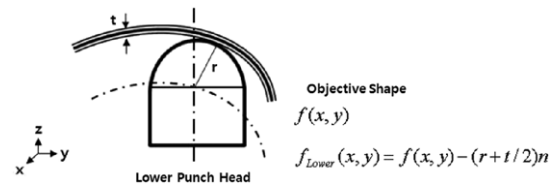
Fig. 5. Surface function of lower punch's head with contact condition.

2. Calculating the normal vector at the contact point.
3. Calculating the surface function of the center of the punch heads.

The region of a punch head projecting onto a workpiece is discretized using dense points as shown in Fig. 5. The location of the closest points is determined as the contact points after the distance between the points on the punch head and the projected point set are calculated.

Since the objective three-dimensional surface of the workpiece to be formed $f(x, y)$ is represented with a polynomial, we can calculate the normal vector ($\mathbf{n}(x, y)$) at the contact points as explained in Eq. (7).

$$\mathbf{n}(x, y) = \frac{f_x(x, y) \times f_y(x, y)}{\left|f_x(x, y) \times f_y(x, y)\right|} \tag{7}$$

where, $f_x(x, y)$ and $f_y(x, y)$ form the differential equation of the polynomial surface $f(x, y)$ expressed by $\frac{\partial f(x,y)}{\partial x}$, $\frac{\partial f(x,y)}{\partial y}$, respectively.

After we obtain the normal vector, the location of the punch heads can be obtained by the following equation:

$$f_{Lower}(x, y) = f(x, y) + (r - t/2)\mathbf{n}. \tag{8}$$

3. Finite element model of deformation process

Using the iterative algorithms, there is a sequential coupling between the FE software and the compensation algorithm as depicted in Fig. 3. Each step of displacement adjustment requires the running of an FE model. In the case of metal forming, this FE analysis must be robust and needs to be sequentially performed.

The forming of hull plates can be defined as the deformation of thick, flat plates into desired surfaces. In many studies, springback is analyzed by an elasto-plastic bending model. If the springback shape is predicted, the results of the prediction can be used in the re-arrangement of the tool in the repeated compensation. Since the deformation component can be divided into bending strains and in-plane strains, the deformation of the MPPF can be modeled by the elasto–plastic deformation of a thick plate. Considering that the finite element model is an efficient method to compute the springback shape, an elasto-plastic shell element capable of large strain and large deformation is adopted. The present method
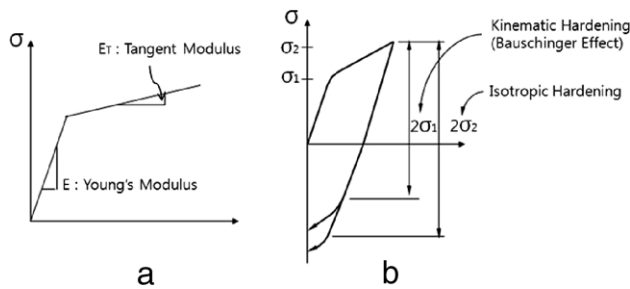
Fig. 6. Stress–strain curve for hardening model.
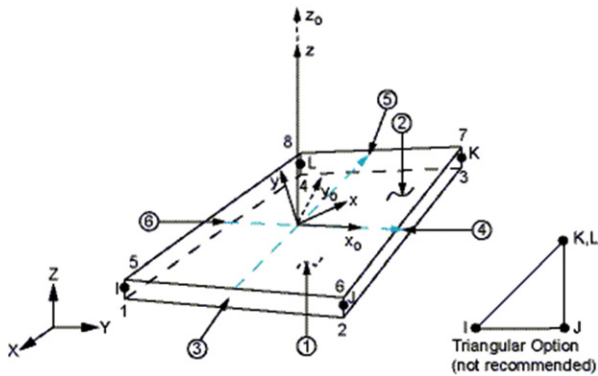
Fig. 7. Typical feature of Shell 181 element.

Table 1
Material property of AH32 TMCP steel.

Material property	Value
Young's modulus (GPa)	210.0
Poisson's ratio	0.3
Yield Stress (MPa)	312.0
Tangent modulus (GPa)	10.0

Fig. 8. Boundary condition at loading stage.

used to compensate for springback involves offsetting the strokes of the pressing punches according to the difference between the desired and the predicted-springback plate. The final strokes can be determined once the error between the designed and predicted shapes converges to a specified tolerance through a number of finite element computations.

3.1. Finite element model

Various investigations have reported that springback is a complex problem which involves plastic strain. Therefore, to accurately model the problem it is preferable to use appropriate models that are capable of describing material behavior such as the Bauschinger effect. The finite element method is a successful way to model the plastic deformation of the multi-point forming procedure. The commercial program ANSYS was used to simulate deformation under various piston stokes. The major conditions of the finite element analysis are given as follows:

- The materials were defined as isotropic and homogenous.
- The kinematic hardening model with the Bauschinger effect was used for strain hardening.
- The thermal effects and friction effects were neglected.

The kinematic hardening rule representing the rigid motion of the yield surface during loading was used, as shown in Fig. 6. It is capable of simulating the load–displacement response, including the Bauschinger effect. The finite element chosen was SHELL181, a plastic-shell element that is suitable for the simulation of shell structures and which permits the incorporation of plastic-elastic behavior according to the requirements of the simulation. The element was a 4-node element with six degrees of freedom at each node: translations (u, v, w) in the x, y, and z directions, and rotations (θ_x, θ_y, θ_z) about the x, y, and z-axes as shown in Fig. 7. This element represents the meshes in three dimensions and needs four or three nodes to be defined [24].

SHELL181 is suitable for analyzing moderately thick shell structures. It is well-suited for linear, large rotation, and/or large strain nonlinear applications. The accuracy in modeling a thick plate is governed by the first order shear deformation theory (usually referred to as the Mindlin–Reissner shell theory). The interpolation of shear strain for the elements is adjusted to avoid shear locking. The problem of large rotations and deflection is treated by considering the shear deformation as well as the nonlinear strain–displacement relationship.
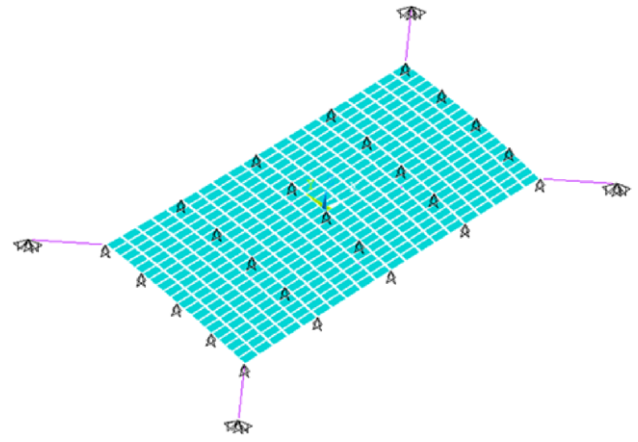
Considering the material properties of the AH32 Thermo Mechanical Controlled Process (TMCP) steel plate, the mechanical properties of the work pieces were assumed as listed in Table 1.

3.2. Boundary conditions

The finite element meshes and the boundary conditions at loading and unloading state are shown in Figs. 8 and 9. If the boundary condition allows the rigid body motion due to the lack of constraints, then the stiffness matrix of the FE model is singular. The mid node was constrained to prevent the rigid body translations and rotations at the loading state as well as the nodes at the vertices were linked with the spring element that was fixed at one end. The displacement constraints of translations and rotations were applied to the mid node of the surface in order to prevent the rigid body motion. This is a stable constraint, preventing all possible rigid body movements, leading to a nonsingular stiffness matrix and thus a successful solution during FEA. Also, the stiffness of the spring element was assumed to be very small so that it only prevented the translation of the meshes without affecting the amount of residual deformation. To simulate the forced displacement that occurs during the forming, an upward displacement (or stroke) was imposed on the inner pressing points. However, the upward displacement was determined by the difference from the mid node because the mid node was fixed.

4. Displacement adjustment

The finite element model described above will provide the springback prediction. The predicted results can then be used in the repeated step of compensation. While many studies for springback compensation have been carried out, the displacement adjustment
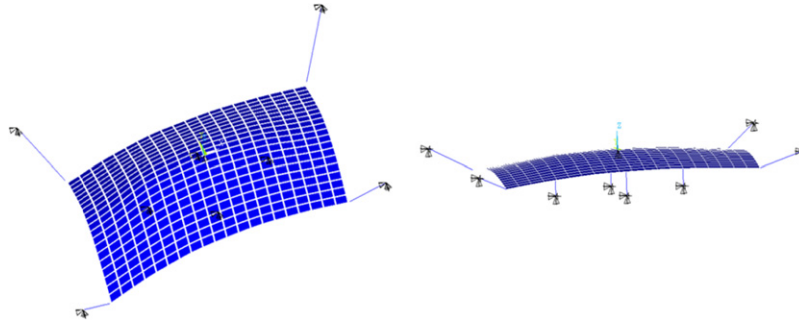
Fig. 9. Boundary condition at unloading stage.

method has been proven to be the most successful [25,26]. The principle behind the DA method is efficiency and repetition. Because the produced surface springs back in a direction, the tool offset is modified into the opposite direction in consideration of the predicted shape. In this chapter, an optimum technique DA is summarized to construct the offset of a multi-point pressing machine. The DA technique is incorporated into the finite element code via the interface to help the construction of the modified offset.

4.1. Constituents of iterative displacement adjustment

The desired surface and unfolding surface were matched or registered based on the ICP as shown in Fig. 3. When the surfaces are registered, press bending needs to be carefully configured and springback compensation must be carried out to improve the geometrical accuracy of the manufactured workpiece. To enhance the iterative manual springback compensation, a finite element analysis was integrated with the displacement algorithm rather than using real prototype tools. The error due to springback is defined as the normal direction from a node of the predicted surface to the desired surface. The details of each step in the DA algorithm are discussed below in detail.

4.2. Displacement adjustment

To date, the DA method has proven to be the most effective and simplest method. The principle behind the method is well known and has already been applied in sheet metal forming. The present study uses the DA algorithm implemented by Lee et al. [10], Lingbeek et al. [14], and Lan et al. [15]. The idea involves measuring the deformed surface and calculating the displacement between the produced surface and the desired shape [14]. Simply, the method compares the deformed surface with the desired surface and calculates the distance between the produced workpiece and the desired surface. The stroke of the presses is then adjusted in the opposite direction to the springback deformation. The same process is iterated until the deviation of displacements satisfies the given tolerance.

The DA method is based upon the iterative compensation computed by the difference between the reference surface and the produced surface. Fig. 10 shows the desired surface, the springback surface at the released state, and the deformed surface at the loading state in the DA method. $\vec{r}_i$ (or **R**), $\vec{s}_i$ (or **S**), and $\vec{c}_i$ (or **C**) represent the desired reference surface, the springback surface, and the compensated surface, respectively. Therefore, $\vec{s}_i - \vec{r}_i$ represents the shape deviation between the desired shape and the deformed shape that experiences the springback. The DA method involves offsetting tool surface nodes in the opposite direction to that of the springback deviation. In the method, the iterative work is applied to the points on the nodes of the finite element mesh and the desired reference surface. The points are given as the collections of
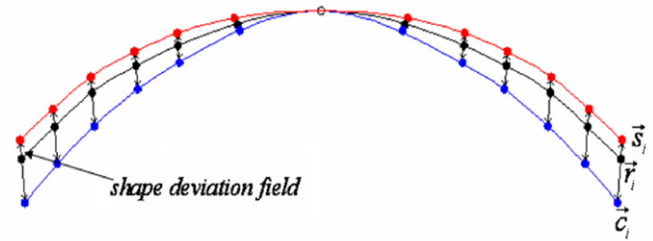
Fig. 10. Sectional view of object surface and sprung back surface.

m points in R^3.

$$S = \{\vec{s}_i | \vec{s}_i \in R^3, 1 \leq i \leq m\} \tag{9}$$

$$R = \{\vec{r}_i | \vec{r}_i \in R^3, 1 \leq i \leq m\}. \tag{10}$$

While the tool's offset is adjusted to compensate for the springback, the amount of springback increases. Therefore, the workpiece must be overbent to accommodate this phenomenon. For this reason, the overbending factor is useful. This fundamental principle is shown in Eq. (11).

Prior to the work of this paper, the DA algorithm was implemented by Lee et al. [10] as an aim of springback compensation, but the implemented DA was performed by iterative manual work. Also, the modification factor was assumed to be a fixed value that was small enough to carefully adjust the stroke in that study. The present study selected the normalized factor to determine the direction as well as the amount of modification. Therefore, the compensated geometry $\mathbf{C}^{t+1}$ after the tth iteration is easily tested by the modification factor ($\boldsymbol{\alpha}$),

$$\mathbf{C}^{t+1} = \mathbf{C}^t + \boldsymbol{\alpha}^t(\mathbf{S} - \mathbf{R}) \Leftrightarrow \vec{c}_i^{t+1} = \vec{c}_i^t + \alpha_i^t(\vec{s}_i^t - \vec{r}_i) \quad \forall i. \tag{11}$$

The factor α_i^t is the scale factor or overbending factor of the ith node at the tth iteration. The amount of compensation varies over the nodes. The scale factor is determined by Eq. (12). This is the normalized value to the maximum deviation at all nodes.

$$\alpha_i^t = -\frac{|s_i^t - r_i|}{\max(|s_i^t - r_i|) \, \forall i}. \tag{12}$$

R is the desired reference surface, represented as a set of points. This geometry is used to create the initial trial of pressing strokes as well as to validate the produced surface. Finite element simulation is carried out in order to provide $\mathbf{S}^t$, the produced surface after springback. The compensated geometry $\mathbf{C}^t$ at the previous step is modified into $\mathbf{C}^{t+1}$. As the pressing rod compresses the workpiece, the forced displacement generates the different degrees of deformation that affect the springback results. The first compensated geometry is referred to as $\mathbf{C}^1$, and FE simulation is carried out for the compensated geometry. The resulting springback mesh $\mathbf{S}^1$ is now used to modify $\mathbf{C}^1$, delivering the second compensated geometry $\mathbf{C}^2$. The initial value of $\boldsymbol{\alpha}$ starts with -1.0 and is re-calculated
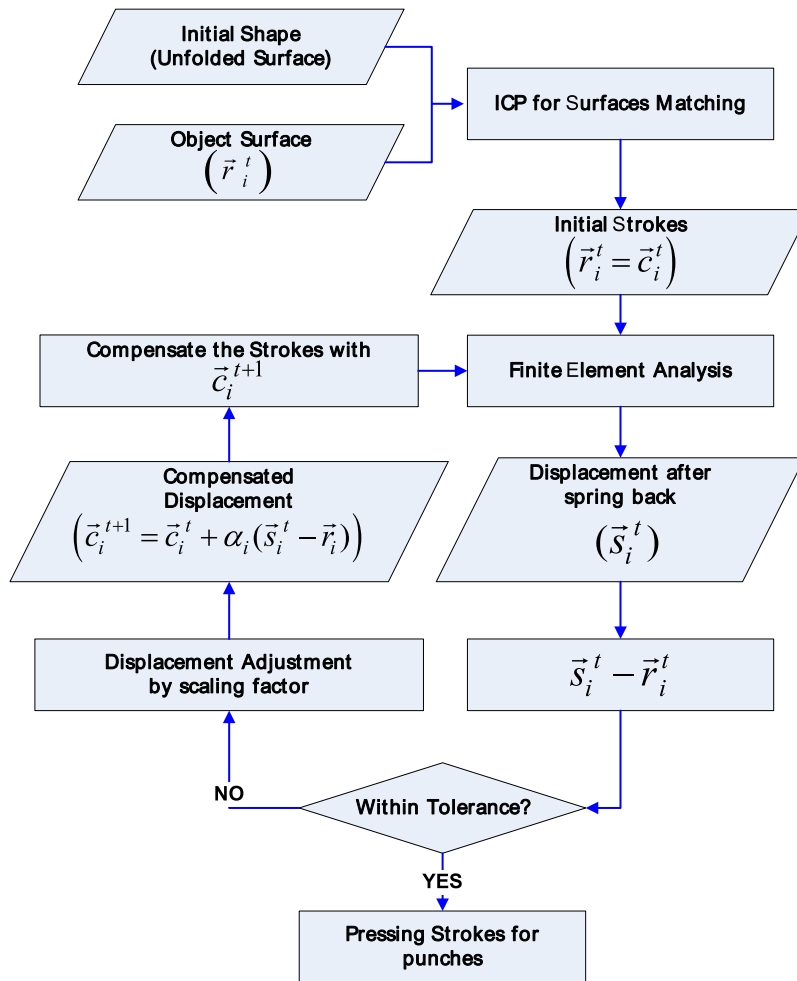
Fig. 11. Sequential procedure for application of the DA.

by Eq. (12). Thereafter, FEA is carried out to calculate the updated $(\mathbf{S}^t)$, calculating the new compensated geometry $(\mathbf{C}^{t+1})$. The iterative process is expressed by a flow chart in Fig. 11.

This process is repeated until the shape deviation satisfies the tolerance criteria,

$$\left\| \vec{s}_i - \vec{r}_i \right\| \le \varepsilon \tag{13}$$

where, ε denotes tolerance.

The advantage of iterative DA is that the process engineer does not need to guess an overbending factor because the tool geometry iteratively converges to its optimal shape. Another advantage is that, depending on the product's geometry and forming process, the accuracy can also be raised [14].

4.3. Integrated system

Despite the powerful capacity of FEA and DA, the tool design process is useless if it still contains manual work. After the studies on the FEA and experiments [27–31] were performed, the focus has now moved towards the integration of FEA and DA [25,32]. Though some studies implemented the integration of DA and FEA and showed the practical approach applicable to the sheet metal forming, it still requires making an integration of the FEA and the DA that can be applied to the formation of the thick plate.

In this study, an approach is introduced to obtain manufacturing information from FE simulation and DA that does not need manual operation until the compensated strokes are obtained. The

DA can be useful only if it is incorporated with the springback calculation. FE analysis should be run during the DA algorithm in an automatic way and the surface data needs to be manipulated as shown in Fig. 12. Finally, software has been developed to calculate the modified strokes automatically, based on the compensation algorithm and finite element method. The integration program in itself is perhaps the most important for industrial use in a shipyard. Combining the FEA with the DA method, this study has developed an integrated system. The integrated software was developed with VISUAL C# under the WINDOWS platform. The software calculates the stroke matrixes and runs the simulation of deformation. With the GUI interface, 3D surface can be constructed based on the input file including four boundary curves. The software controls the iterative adjustment and finite element analysis as well as automatically registers the unfolding surface to the desired shape based on the ICP during the iteration, as illustrated in Fig. 13. At every iteration, the integrated system generates the ANSYS command file corresponding to the compensated displacement of the pressing rods and executes the ANSYS program for the command file in a batch mode. Depending on the object workpiece, the aforementioned tool properties, boundary conditions and workpieces are generated in the FE model. Derived from the calculated deformations, the DA is applied to the deformed shape and a new die surface is obtained after a few iterations. The springback shape is thereby iteratively computed in the integrated system. Consequently, the entire process automatically continues to adjust the spring shape until the forming deviation satisfies the convergence tolerance.
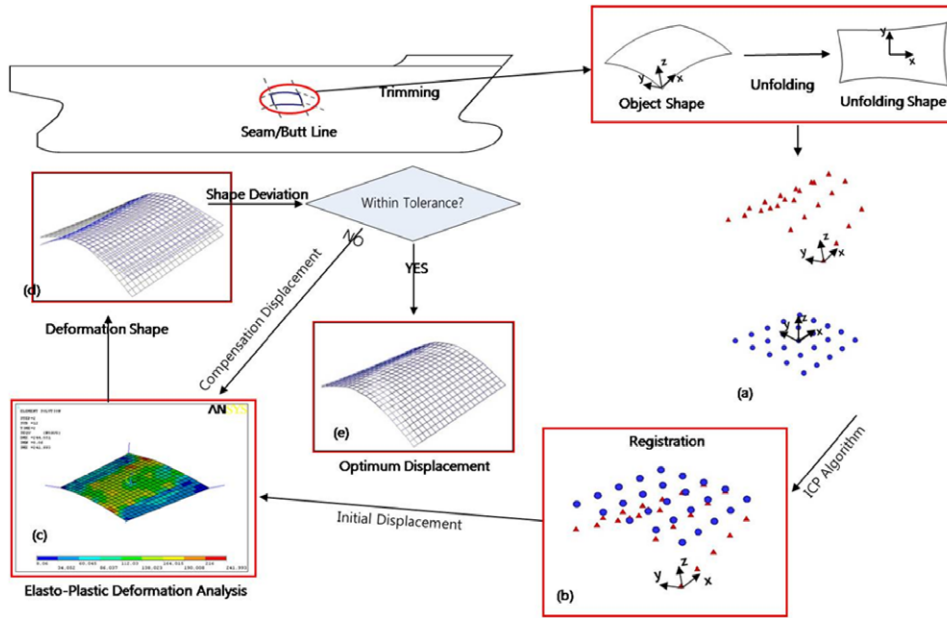
Fig. 12. Data flow for application of the DA.
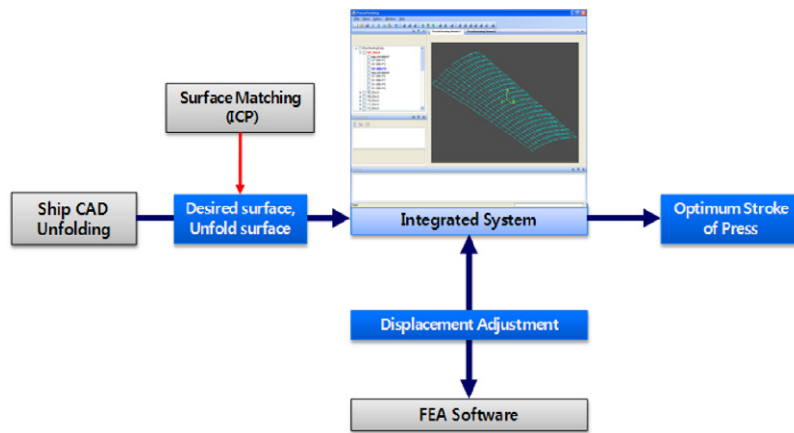
Fig. 13. Configuration of program integrating the ICP, DA, and FEA.

5. Examples and discussions

To check the effectiveness of the proposed method for the direct generation of the offset, several case examples are calculated. The method is applied to compound surfaces extracted from the 2800-TEU container carrier designed by the STX shipyard. Real pieces are selected from the bow and the stern area on the hull form, which have complex curvature distributions. Table 2 provides the dimensions and types of each design surface.

Extracted design surfaces were processed in order to obtain the initial flat plate through the unfolding method [17]. The deformed surface, design surface and pressing surface of each case are shown in Figs. 14, 16, 18, 20, 22 and 24. The shape deviations before and after compensation are pictured in the figures. In addition, the number of iterations and the changes of similarity are shown in Figs. 15, 17, 19, 21, 23 and 25. The similarity (shape deviation) during the iterative compensation was also plotted. The iteration was programmed to stop when 90% of the points fell within the shape difference tolerance of 7 mm. Case 5 and Case 6 required more iterations to converge than did the other cases. The main reason for this is the sizes of the destination surfaces involved. Since the plate sizes of Case 5 and Case 6 were larger than those of the other cases, these cases required more iterative compensation.
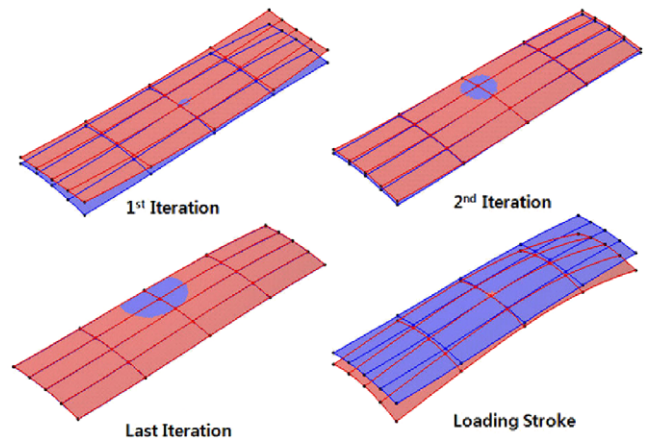
Fig. 14. Deformed shape at each iteration (Case 1).

For this experiment, it was assumed that there were 25 pressing points for all cases. The fact that more iterations were required for the larger plates indicates that pressing points should be added if the size of the plate surface to be altered exceeds a critical value.

Table 2
Sample plates for numerical evaluation.

Design surface	Type	Position	length (mm)	width (mm)	thickness (mm)
Case 1	Convex	Stern	4015.11	1133.09	20
Case 2	Convex	Stern	3928.88	1016.27	20
Case 3	Saddle	Bow	1752.39	1042.82	20
Case 4	Saddle	Bow	1221.83	508.78	20
Case 5	Twist	Stern	6881.73	2466.29	20
Case 6	Twist	Stern	5931.18	1643.39	20
Case 7	Twist	Bow	1880.0	1003.0	20
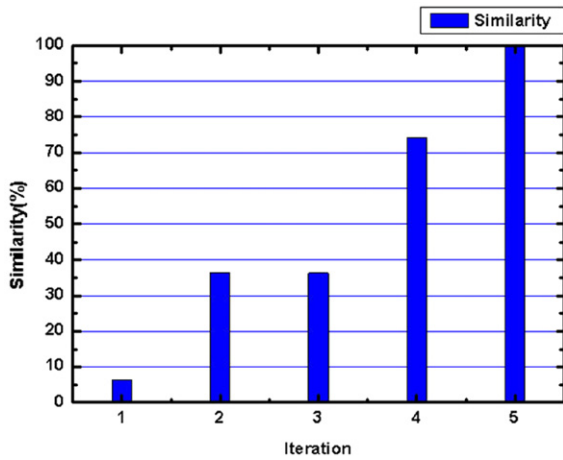
Fig. 15. Similarity at each iteration (Case 1).
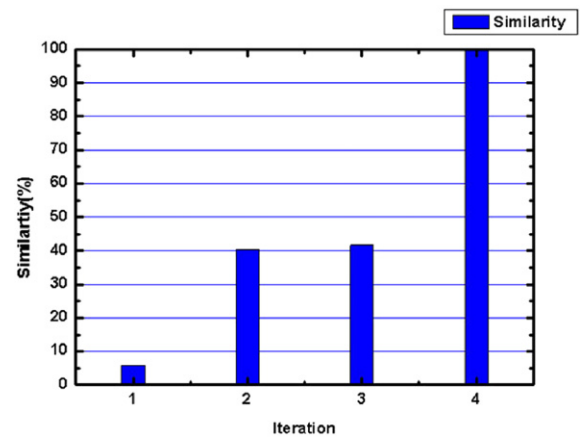
Fig. 17. Similarity at each iteration (Case 2).
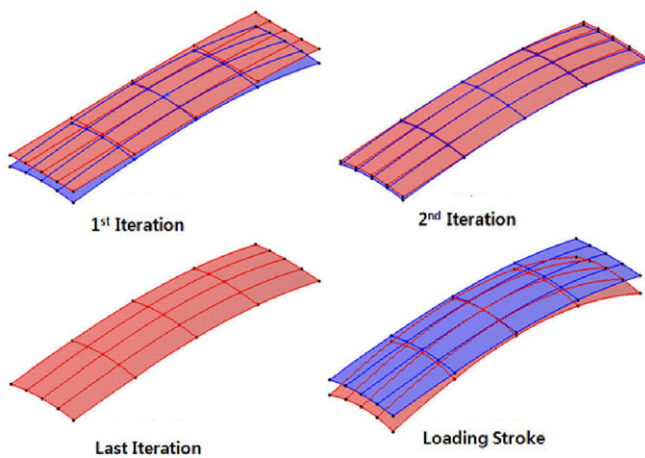
Fig. 16. Deformed shape at each iteration (Case 2).
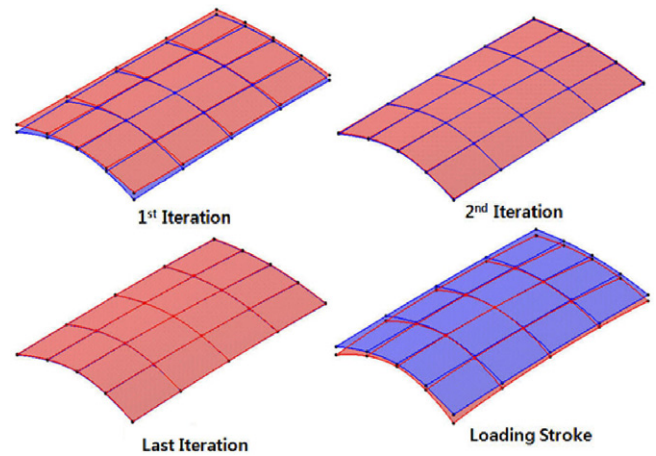
Fig. 18. Deformed shape at each iteration (Case 3).

Furthermore, pressing points should be rearranged according to the curvature distribution of the design surface. The convergence of a large plate can be improved by adding more pressing points.

Although the similarity of Cases 1–4 increases with the iteration cycles, that of Case 5 and Case 6 decreases with the cycles, and then increases again. This tendency is found in most of the twist type surface. A hypothesis is that the twist type surface has the vertices located in the opposite direction, while the compensation factor is a relatively normalized value to the maximum difference. The twist type surface has the vertices located in the opposite direction with respect to the mid node. In the Convex (Case 1–2) or Saddle (Case 3–4) type, four vertexes are located at the same direction with respect to the mid node. As stated earlier in the Section 3.2, the stroke of each node was determined by the vertical distance with respect to the mid node because the mid node was fixed to prevent the rigid body translation during the finite element analysis. Furthermore, the local compensation
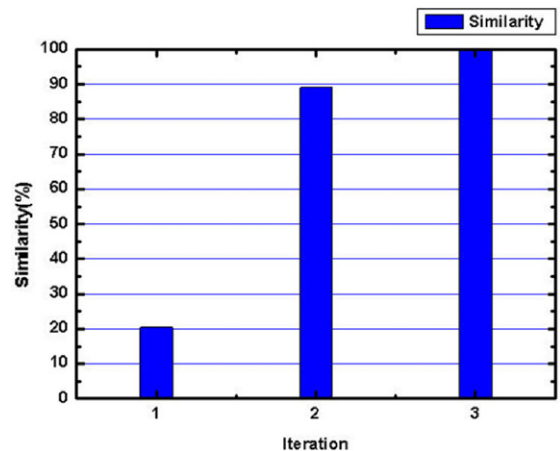
Fig. 19. Similarity at each iteration (Case 3).
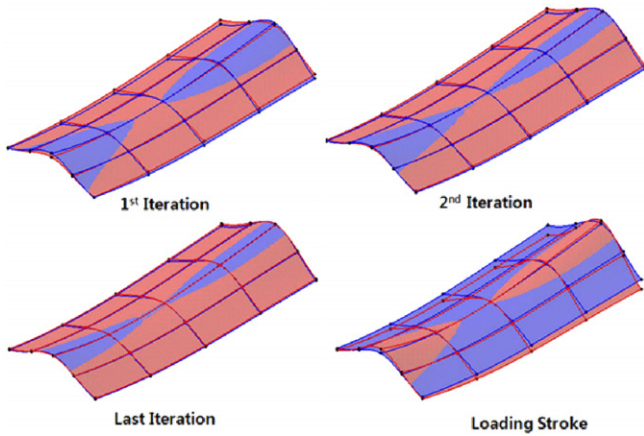
Fig. 20. Deformed shape at each iteration (Case 4).
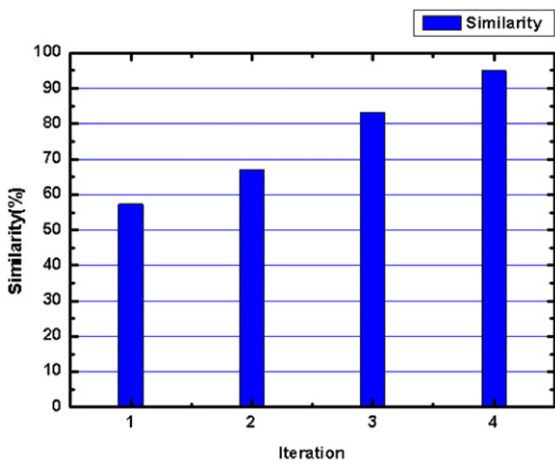
Fig. 21. Similarity at each iteration (Case 4).
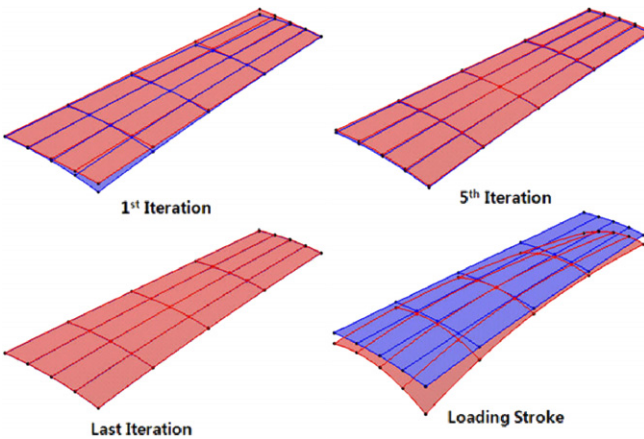
Fig. 22. Deformed shape at each iteration (Case 5).
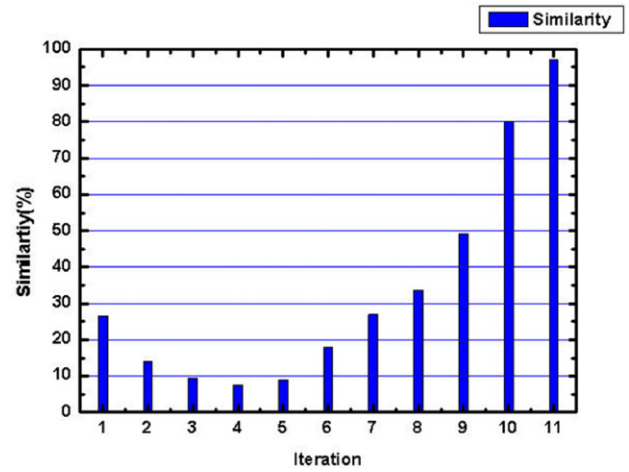
Fig. 23. Similarity at each iteration (Case 5).
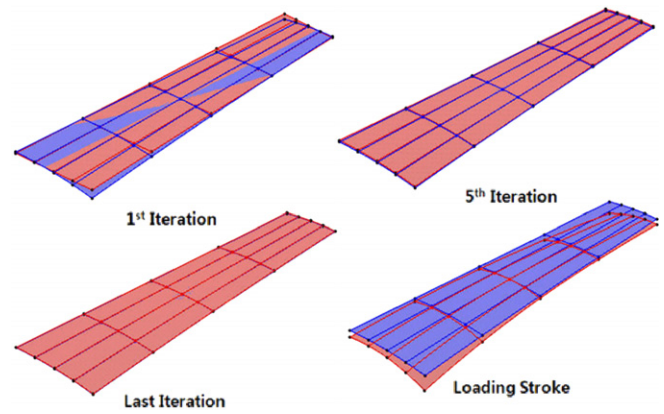
Fig. 24. Deformed shape at each iteration (Case 6).
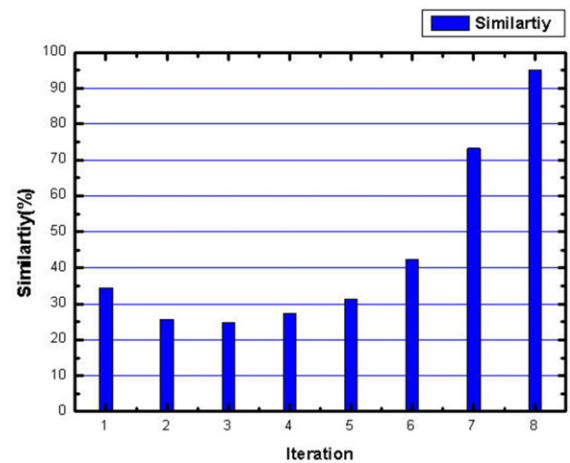
Fig. 25. Similarity at each iteration (Case 6).

factor α is determined by the ratio to the maximum deviation between the mid node and the other nodes as explained in Eq. (12). To investigate the effectiveness of the size on the convergence, another calculation is carried out. Figs. 26 and 27 show the result of the twist surface that is smaller than Case 5–6. It is found that the convergence is getting better if the size of plate is small even in case of the twist type surface. Although it is difficult to explain the cause of similarity fluctuation found in the twist surfaces, it can be concluded that the convergence of DA is affected by the size of and the type of the surface.

6. Conclusions

In recent years, cold forming has been an attractive process used in shipyards. MPPF technology employs one set of adjustable punch matrices to take the place of fixed-dies. During the forming process, each of the punches can be controlled by hydraulic pressure to adjust its coordinates for shaping discrete 3D punch surfaces. Based on the MPPF methodology, a single side multi-point dieless tool is being developed by the STX shipyard. The main
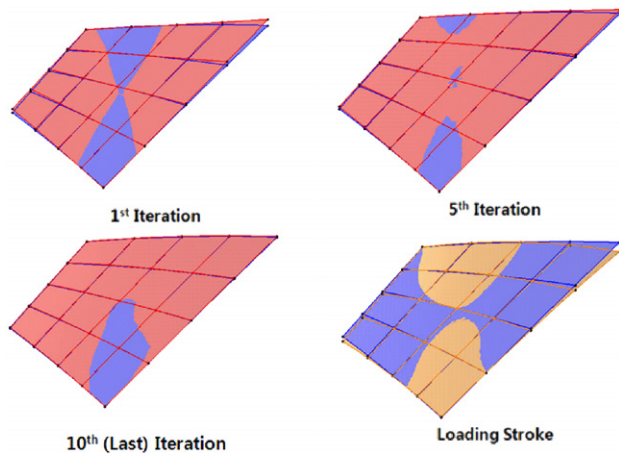
Fig. 26. Deformed shape at each iteration (Case 7).
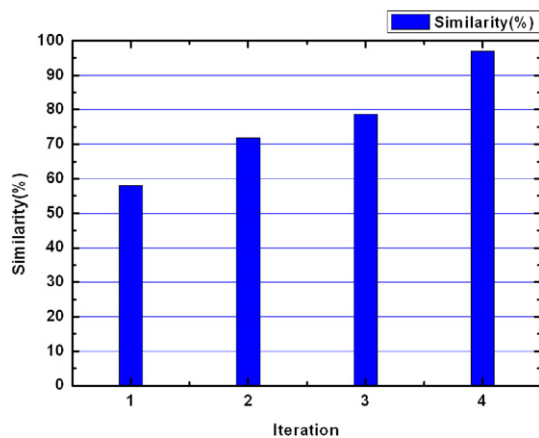
Fig. 27. Similarity at each iteration (Case 7).

contribution of this paper is to develop an integrated system for thick plate forming performed by the single side MPPF. Firstly, this paper introduces the principles of the springback compensation method. It then describes in detail the construction of the flexible information system. The system combines the configuration of MPPF tooling, multi-point position and FEA to achieve the flexible forming and rapid calculation of punch strokes.

To determine the piston strokes in multi-point forming from a set of scattered data points, the compensated position of each piston point should be calculated. To accomplish this calculation, an integrated displacement compensation method which combines ICP, DA, and FEA has been proposed in this study. In the proposed method, design surfaces and unfolded surfaces from a set of scattered data points are matched together by the ICP and localization algorithm. ICP and localization register the unfolded surfaces onto the curved design surfaces. To offset the piston strokes in multi point forming from a set of scattered data points, the compensated position of each piston point is calculated by DA. An integrated IDM system has also been developed to automatically calculate the compensation strokes necessary for all hull plates. The integrated IDM system successfully generates appropriate compensated strokes for the pistons during multi-point forming. The DA method is incorporated into a commercial FE code through a batch-run interface to repeat the iterative compensation by the integrated system. Calculating the elastic–plastic deformation using a plastic shell element, piston stroke variations are optimized to produce the desired plate shape.

The main conclusions from the present work are as follows:

- The method has been proven effective in compensating for springback during thick plate forming in shipbuilding.
- A numerical example demonstrates that the combination of DA and FEA is easy and expedient to apply to hull forming.
- The density of the piston grid is one of the major factors in multi-point forming. The convergence of IDM decreases when the size of the plate is enlarged.

Acknowledgement

References

[1] Son KJ, Yun JO, Kim YW, Yang YS. Analysis of angular distortion in line-heating. International Journal of Mechanical Sciences 2007;49(10):1122–9.
[2] Shin JG, Lee JH. Nondimensionalized relationship between heating conditions and residual deformations in the line heating process. Journal of Ship Research 2002;46(4):229–38.
[3] Suhara T. Study of thermo plastic working: Bending of beam of rectangular cross section. Journal of Zosen Kyokai 1958;103:233–43 [in Japanese].
[4] Iwamura Y, Rybicki EF. A transient elastic–plastic thermal stress analysis of flame forming. Transactions of the Japan Welding Society 1973;4(2):189–98.
[5] Nomoto T, Ohmori T, Sutoh T, Enosawa M, Aoyama K, Saitoh M. Development of simulator for plate bending by line-heating. Journal of The Society of Naval Architects of Japan 1990;168:527–35 [in Japanese].
[6] Tango Y, Ishiyama M, Nagahara S, Nagashima T, Kobayashi J. Automated line heating for plate forming by IHI-ALPHA system and its application to construction of actual vessels—System outline and application record to date. Journal of the Society of Naval Architects of Japan 2003;193:85–95.
[7] Jang CD, Kim HK, Ha YS. Prediction of plate bending by high-frequency induction heating. Journal of Ship Production 2002;18(4):226–36.
[8] Shin JG, Ryu CH, Lee JH, Kim WD. A user-friendly, advanced line heating automation for accurate plate fabrication. Journal of Ship Production 2003;19(1):8–15.
[9] Park JS, Shin JG, Ko KH. Geometric assessment for fabrication of large hull pieces in shipbuilding. Computer-Aided Design 2007;39(10):870–81.
[10] Lee JH, Yoon JS, Ryu CH, Kim SH. Springback compensation based on finite element for multi-point forming in shipbuilding. Advanced Materials Research 2007;26–28:981–4.
[11] Shim DS, Yang DY, Kim KH, Han MS, Chung SW. Numerical and experimental investigation into cold incremental rolling of doubly curved plates for process design of a new LARS (line array roll set) rolling process. CIRP Annals - Manufacturing Technology 2009;58:239–42.
[12] Li MZ, Cai ZY, Sui Z, Yan QG. Multi-point forming technology for sheet metal. Journal of Material Processing Technology 2002;129:333–8.
[13] Huang X, Gu P. CAD-model based inspection of sculptured surfaces with datums. International Journal of Production Research 1998;36(5):1351–67.
[14] Lingbeek R, Huetink J, Ohnimus S, Petzolt M, Weiher J. The development of a finite elements based springback compensation tool for sheet metal products. Journal of Materials Processing Technology 2005;169:115–25.
[15] Lan F, Chen J, Lin J. A method of constructing smooth tool surface for FE prediction of springback in sheet metal forming. Journal of Materials Processing Technology 2006;177:382–5.
[16] Pérez-Arribas F, Suárez-Suárez JA, Fernández-Jambrina L. Automatic surface modelling of a ship hull. Computer-Aided Design 2006;38:584–94.
[17] Ryu CH, Shin JG. Optimal approximated unfolding of general curved shell plates based on deformation theory. Journal of Manufacturing Science and Engineering 2006;128(1):261–9.
[18] Huang X, Gu P, Zernicke R. Localization and comparison of two free-form surfaces. Computer-Aided Design 1996;28(12):1017–22.
[19] Faugeras OD, Hebert M. The representation, recognition and locating of 3-D objects. International journal of Robotic Research 1986;5(3):27–52.
[20] Horn BKP. Closed-form solution of absolute orientation using unit quarternions. Journal of Optical Society of America 1987;4(4):629–42.
[21] Besl PJ, Mcday ND. A method for registration of 3-D Shapes. IEEE Transactions on Pattern Analysis and Machine Intelligence 1992;14(2):239–56.
[22] Rusinkiewicz S, Levoy M. Efficient variants of the ICP algorithm. Third International Conference on 3-D Digital Imaging and Modeling 2001;145–52.
[23] Cai ZY, Li MZ. Optimum path forming technique for sheet metal and its realization in multi-point forming. Journal of Materials Processing Technology 2001;110:136–41.
[24] ANSYS. Theory manual. ANSYS Co., Ltd. 2007.

[25] Meinders T, Burchitz IA, Bonte MHA, Lingbeek RA. Numerical product design: Springback prediction, compensation and optimization. International Journal of Machine Tools & Manufacturer 2008;48:499–514.
[26] Gan W, Wagoner RH. Die design method for sheet springback. International Journal of Mechanical Science 2004;46:1097–113.
[27] Huang Y, Chen T. An elasto-plastic finite-element analysis of sheet metal camber process. Journal of Materials Processing Technology 2003;140(1–3): 432–40.
[28] Lei L, Hwang S, Kang B. Finite element analysis and design in stainless steel sheet forming and its experimental comparison. Journal of Materials Processing Technology 2001;110(1):70–7.
[29] Tekiner Z. An experimental study on the examination of springback of sheet metals with several thicknesses and properties in bending dies. Journal of Materials Processing Technology 2004;145(1):109–17.
[30] Ueda M, Ueno K, Kobayashi M. A Study of springback in the stretch bending of channels. Journal of Mechanical Working Technology 1981;5:163–79.
[31] Cai ZY, Li MZ. Finite element simulation of multi-point sheet forming process based on implicit scheme. Journal of Materials Processing Technology 2005; 161(3):449–55.
[32] Lui C, Li M, Fu W. Principles and apparatus of multi-point forming for sheet metal. Journal of Advanced Manufacturing Technology 2008;35: 1227–333.